THE ASTROPHYSICAL JOURNAL, 490:194–201, 1997 November 20

THE BUTCHER-OEMLER EFFECT IN ABELL 2317

KARL D. RAKOS[1,2]
Institute for Astronomy, University of Vienna, A-1180, Wein, Austria; rakosch@astro1.ast.univie.ac.at
ANDREW P. ODELL[2]
Department of Physics and Astronomy, Northern Arizona University, Box 6010, Flagstaff, AZ 86011; andy.odell@nau.edu
AND
JAMES M. SCHOMBERT[1]
Department of Physics, University of Oregon, Eugene, OR 97403; js@abyss.uoregon.edu
Received 1997 February 26; accepted 1997 June 30

ABSTRACT

This paper presents deep narrowband photometry of the cluster A2317 ($z = 0.211$) carried out using the KPNO 4 m and Steward 2.3 m telescopes. Using rest frame Strömgren photometry, it is determined that A2317 has an unusually high fraction of blue galaxies (the Butcher-Oemler effect) for its redshift ($f_B = 0.35$). We demonstrate that the ratio of blue to red galaxies has a strong dependence on absolute magnitude such that blue galaxies dominate the top of the luminosity function. Spectrophotometric classification shows that a majority of the red galaxies are E/S0's, with a small number of reddened starburst galaxies. Butcher-Oemler galaxies are shown to be galaxies with star formation rates typical of late-type spirals and to be irregular. Starburst systems were typically found to be on the lower end of the cluster luminosity function. In addition, blue galaxies are preferentially found in the outer edges of the cluster, whereas the red galaxies are concentrated in the cluster core.

Subject headings: galaxies: clusters: individual (A2317) — galaxies: photometry — galaxies: stellar content

1. INTRODUCTION

Galaxy evolution has been a rapidly changing field in the last decade primarily because of the great increase in observational information from the *Hubble Space Telescope* (*HST*) and the new generation of 8 m+ class ground-based telescopes (see Ellis 1997 for a review). Early expectations from color evolution models were that strong color evolution would only be visible in galaxies beyond $z = 1$ and, thus, not within the realm of optical telescopes becaue of redshift effects. However, two very surprising facts came to light in the mid-1980s: (1) the discovery of the Butcher-Oemler effect, which is the sharp rise in the fraction of blue cluster galaxies at intermediate redshifts ($z = 0.2$–0.4) (Butcher & Oemler 1984), and (2) the excess of low-luminosity blue galaxies in the field population at intermediate redshifts (Koo 1986; Tyson 1988). These two discoveries indicated that galaxy evolution was more than a simple calculation of color changes from a passively evolving stellar population. There are also significant changes in the star formation history, which result in global changes to the cluster luminosity function and population.

In an earlier paper in this series (Rakos & Schombert 1995; hereafter RS95), we used a rest frame, four-color photometry system (the Strömgren system) to explore the color evolution of 17 clusters of galaxies from redshifts of 0.2 to 0.9. In that paper, the red population was shown to follow closely the passive evolution models for a single burst population with an epoch of galaxy formation near $z = 5$. On the other hand, the blue galaxies (the Butcher-Oemler population) showed a dramatic increase from 20% at $z = 0.4$ to 80% at $z = 0.9$, an even more rapid trend than an extrapolation from intermediate redshift clusters would have predicted. Rakos & Schombert (1995) interpreted this trend as the rapid change of star-forming disk galaxies into quiescent S0's or low surface brightness (LSB) galaxies.

The rapid rise of the blue galaxies in the Butcher-Oemler effect indicates that a majority of a cluster's population is involved in some amount of star formation at epochs less than $z = 1$. Since our results for the red population (ellipticals) are consistent with a formation epoch of $z = 5$, then either all the nonellipticals in clusters (S0's, spirals, and irregulars) are star-forming at $z = 1$, which then slowly discontinue star formation by gas depletion or stripping, or else many of the members of the blue population simply cease to exist by the present epoch. The next stage in our research toward resolving this dilemma is to determine the nature of Butcher-Oemler galaxies.

Our previous observations focused on the brightest galaxies in our cluster sample because of limitations set by the amount of observing time and aperture size. To explore the behavior of the red E/S0's and blue Butcher-Oemler populations in more detail, we decided to return to one of the RS95 clusters with a high fraction of blue galaxies, f_B, and image the cluster members to greater magnitude depth. To this end we have selected an intermediate redshift cluster, Abell 2317, for study. Our goal is to apply our new narrowband, photometric classification system to the blue and red populations in a Butcher-Oemler cluster to (1) illuminate the types of galaxies involved in the Butcher-Oemler effect, (2) determine the dominance of the Butcher-Oemler galaxies to the cluster luminosity function, and (3) examine the spatial extend of the blue and red populations. Values of $H_0 = 50$ km s^{-1} Mpc^{-1} and $q_0 = 0$ were used throughout this paper.

[1] Visiting Astronomer, Kitt Peak National Observatory, National Optical Astronomy Observatories, which is operated by the Association of Universities for Research in Astronomy, Inc. (AURA) under cooperative agreement with the National Science Foundation.
[2] Visiting Astronomer, Steward Observatory, University of Arizona.

2. OBSERVATIONS

Abell 2317 is a high declination cluster ($19^h08^m.5$, $+68°59'.0$) with a redshift of 0.211. The cluster is Coma-like in its richness (richness class 3; Abell, Corwin, & Olowin 1989) and compact with a Bautz-Morgan class of II. The brightest cluster member has an apparent magnitude of 17.3 AB, and the cluster has a moderate Galactic extinction of 0.32.

The observing procedure and reduction used herein is similar to that described in RS95. The observations of A2317 were taken with the KPNO 4 m PFCCD Te1K (binned 2 × 2) in 1991 June and with the Steward Observatory 2.3 m in 1995 July. The scale of the 4 m telescope was $0''.96$ pixel^{-1}, and the exposure time was 25 minutes per filter divided into five frames of 300 s for cosmic-ray subtraction and flattening. The observations on the Steward 2.3 m were restricted to the UV filter mostly to increase the S/N for faint galaxies, since the QE of the 4 m CCD was relatively poor in the blue spectral region. The total exposure time on the 2.3 m was 3 hr divided into frames of 900 s.

Photometry using 32 kpc apertures was performed on the final, co-added frames. Objects were selected based on detection in all four filters at the 3 σ level. There is no evidence from the color-magnitude diagrams that this introduced a color bias to the sample. Incompleteness is evident below $m_{5500} = 20$; the faintest objects are $m_{5500} = 21$. The *yz* magnitudes were calibrated to a 5500 Å luminosity using spectrophotometric standards (see below). Typical errors were 0.02 mag for the brightest cluster members to 0.08 mag for objects below $m_{5500} = 20$.

According to Abell et al. (1989), the size of the cluster is 15.2 × 32.6 mm on the Palomar Sky Survey, which corresponds to $\sim 15' \times 32'$. Our observations cover only the inner $8' \times 8'$ as restricted by the CCD field of view. Four-color photometry in our modified Strömgren system (*uz*, *vz*, *bz*, *yz*; see RS95) was obtained for 200 objects. Each of these filters is ~200 Å wide and was specially designed so that they are "redshifted" to the cluster wavelength in order to maintain a rest frame color system. This provides a photometric system of determining cluster membership without the use of redshift information resulting from the unique shape of any galaxy's spectra around the 4000 Å break. Our method, including the negligible effects from the cluster velocity dispersion, is fully discussed in Rakos, Schombert, & Kreidl (1990) and Fiala, Rakos, & Stockton (1986).

Using our photometric selection criteria, 112 objects (56%) were determined to be cluster members based on the behavior of the *mz* index, which is a measure of the spectral energy distribution (SED) around the 4000 Å break. The *mz* index has the advantage of being relatively flat within ± 3000 km s^{-1} of the cluster redshift with sharp falloffs outside this redshift range. This maximizes the confidence of the membership of detected objects, while minimizing the contamination from nearby field galaxies. The remaining 44% of the observed galaxies belong to the foreground or background contamination, which is in agreement with the expectations from the luminosity function of field galaxies in this magnitude range (Donnelly 1994).

In addition to resolving cluster membership, our four-color photometry system can also be used to produce a photometric classification of galaxy type. This classification is based on the 4000 Å colors (i.e., star formation/activity) and only maps into morphology as one would expect star formation history to map onto the Hubble sequence. In Rakos, Maindl, & Schombert (1996; hereafter RMS96), 140 high-resolution, high-S/N spectra of galaxies were selected from the literature and reduced into synthetic colors in our *uz*, *vz*, *bz*, *yz* system. From these colors, it was demonstrated that two-color and *mz*-color diagrams could be used to classify galaxies into four simple types (ellipticals/S0's, spirals/irregulars, Seyfert galaxies, and starburst galaxies) in a purely spectrophotometric manner (see Fig. 4 of RMS96). Guided by the synthetic color results of RMS96, we have defined our photometric classifications in the following manner (see Figs. 1 and 2). Any galaxy with a red ($vz - yz$) color (i.e., $vz - yz > 0.65$) and *mz* index greater than -0.16 was classified as an E/S0 (an old stellar population object). The boundary between red spirals (Sa's) and E/S0's was clearly defined at $(vz - yz) = 0.65$ in RMS96 and is adopted herein. Any galaxy with a *mz* index less than -0.16 is classified as a starburst. A galaxy that lies within 0.05 mag of the normal star-forming galaxy sequence defined by Figure 3 of RMS96 was classified as a spiral/irregular (a galaxy with a normal star formation rate). And, last, any galaxy that lies 3 σ blueward of the two-color sequence and has a red *mz* index (which is indicative of the presence of strong non–star-forming emission lines typical of active galactic nucleus [AGN] activity) is assigned a Seyfert classification.

The regions with the greatest uncertainty in photometric classification are the boundaries between red spirals and ellipticals/S0's, the upper bound of starbursts, and the lower bound on Seyfert classification. The overlap between red spirals and elliptical/S0's has a minimal impact on our results, since red spirals are primarily large bulge-to-disk, gas-poor objects, similar to S0's themselves. Many evolutionary scenarios depict early-type spirals as evolving to S0's after gas depletion and subsequent reddening of the underlying stellar population. The separation between starbursts and spirals/irregulars is mostly a measure of the degree of global star formation. For the purposes of this study, the classification of starburst has been conservative—the larger the separation from the spiral/

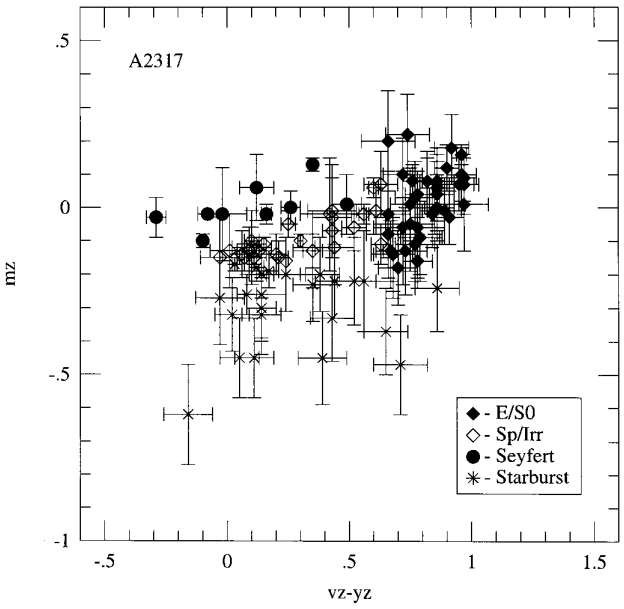

FIG. 1.—The *mz* index vs. metallicity color ($vz - yz$). Photometric classifications are shown. All starburst systems are defined by *mz* indices less than -0.16.

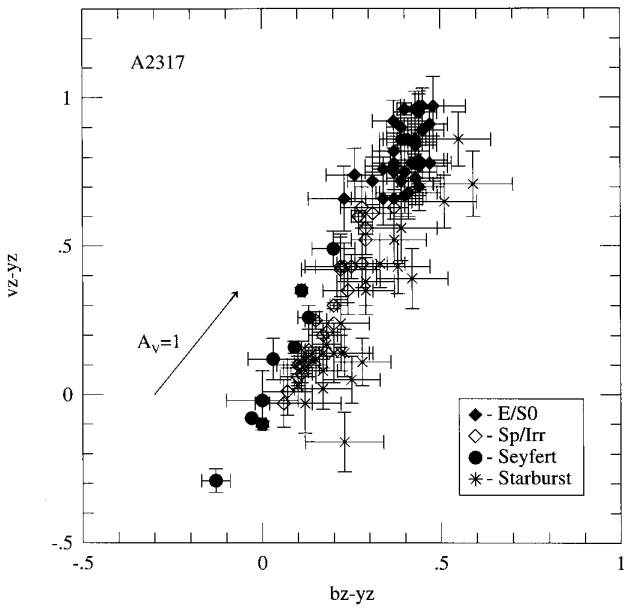

FIG. 2.—Two-color diagram for A2317 members. Photometric classifications are shown. Seyfert galaxies are defined by being bluer than more than 3 σ from the Sp/Irr sequence. A reddening vector of 1 mag is shown. Note that all starburst systems display from 1 to 3 mag of reddening, most probably an IRAS style of starburst shrouded in dust.

irregular midline, the greater the reddening, not the strength of the starburst.

In addition to the colors, the *yz* filter values can be converted to m_{5500}. The Strömgren system was originally designed only as a color system; however, the *yz* filter is centered on 5500 Å, and it is possible to link the *yz* flux to a photon magnitude (i.e., the AB79 system of Oke & Gunn 1983) through the use of spectrophotometry standards. This procedure was described in detail in Rakos, Fiala, & Schombert (1988) and is used to determine the m_{5500} values for all the cluster members. The incompleteness of the sample is not serious until below $m_{5500} = 20$, which corresponds to $M_B = -20.7$ ($H_0 = 50$). The number of fainter galaxies is, in reality, much larger than in our sample, but our results will only depend on the bright end of the luminosity function. In order to save space and publication charges, the data for the 112 cluster members of A2317 are not printed here but can be obtained from the authors in computer-readable format. This ASCII file contains pixel coordinates, m_{5500}, *uz*, *vz*, *bz*, and *yz* colors, errors, and our photometric classifications.

3. DISCUSSION

3.1. *Photometric Classification*

The extragalactic meaning of the Strömgren colors are described in detail in our previous papers (see RS95). Briefly, the Strömgren colors, centered on the 4000 Å break, are crude estimators of recent star formation, mean age, and metallicity. In previous papers, we have used ($vz - yz$) as a measure of global metallicity and ($bz - yz$) as a measure of the mean age of the underlying stellar population. However, precise understanding of these colors requires comparison to SED models with various assumptions (e.g., redshift of formation, mean metallicity, and IMF), since varying star formation histories inhibit a unique interpretation of the colors. Recent star formation can also strongly influence ($vz - yz$), and in this paper we are expanding the use of our Strömgren filters to explore the star formation history of Butcher-Oemler galaxies.

One advantage of the Strömgren colors (or any 4000 Å color system) is their strong dependence on recent star formation and their sensitivity to deviations in star formation rates that signal starburst activity. Rakos et al. (1996) outline the *uvby* system sensitive to star formation with the starburst models of Lehnert & Heckman (1996; see Fig. 6 of RMS96). As discussed in § 2, we have classified the cluster members based on their colors and *mz* indices by a prescription developed in RMS96. We have divided the photometric classifications into four subtypes as current colors reflect into star formation history: (1) elliptical/S0 (E/S0), (2) spiral/irregular (Sp/Irr), (3) starburst, and (4) Seyfert. Operationally, this subtypes are defined as (1) red, non–star-forming colors, (2) blue star-forming colors as defined by Hubble types Sa to Irr, (3) having deviant colors indicative of strong star formation combined with reddening, and (4) peculiar fluxes in the *vz* filter that signal the AGN phenomenon. The relationships between galaxy type and color indices are shown in Figures 1 and 2, which are the *mz*-color and two-color diagrams.

Starburst galaxies cover a range of colors from blue to red but are located on the reddened side of the two-color diagram. The analysis of interacting and merging galaxies in RMS96 demonstrated that the typical colors of a tidally induced starburst system lie in this portion of the two-color diagram (Fig. 2). It is possible to differentiate between starburst galaxies shrouded in dust with strong reddening (IRAS starbursts; Lehnert & Heckman 1996) and the strong ultraviolet radiation of Wolf-Rayet galaxies simply by the distance the galaxy lies from the Sp/Irr sequence along the reddening line, although the exact amount of reddening is subjective. The reddening line in Figure 2 indicates that a majority of the starburst galaxies have Sb or later colors with significant extinction by dust.

The reader is cautioned that this classification scheme is based on the integrated colors and is not a morphological system. The designation of E/S0, Sp/Irr, or starburst only refers to the current star formation rate and recent SF history of the galaxy, not to its morphological appearance, the existence of spiral arms, or a bulge-to-disk ratio. For example, there is no discrimination between ellipticals and S0's, since their global colors are identical. Many of the galaxies on the blue side of the E/S0 boundary may, in fact, be large-bulge Sa's whose blue disk light is overwhelmed by the more dominant red bulge. Galaxies on the red side of the Sp/Irr sequence may be the new class of "E + A" post-starburst galaxies whose smooth morphology is not measured or may be simply disk systems with very low star formation rates. However, there has always been a strong relationship between galaxy color and morphology such that it can be assumed that a majority of the Sp/Irr systems, classified by color, are disk galaxies. Likewise, the starburst systems are most likely interacting or merging galaxies, and Seyfert galaxies are disk galaxies with AGN cores.

Judging from the results of the photometric classification, A2317 is similar to other Butcher-Oemler clusters in being deficient in E/S0's and overabundant in late-type galaxies. The population fractions are listed in Table 1 and, in particular, we find that 47 (42%) of the cluster members are E/S0's, whereas 29 (26%) are Sp/Irr, and 25 (22%) are starbursts. The remaining 11 (10%) are classified as Seyfert galaxies. Typical E:S0:Sp/Irr ratios for present-day clusters

TABLE 1

A2317 CLUSTER POPULATION

Type	Blue	Red	Total
E/S0.....	0 (0%)	47 (64%)	47 (42%)
Sp/Irr	18 (46%)	11 (15%)	29 (26%)
Seyfert	11 (29%)	0 (0%)	11 (10%)
Starburst.....	10 (25%)	15 (21%)	25 (22%)
Total	39 (35%)	73 (65%)	112

are 20%/40%/40% (Oemler 1992), based on morphological classification of the nearby cluster galaxies. It is assumed that all the galaxies photometrically classified as Sp/Irr, starburst, and Seyfert would be contained in a late-type category and, thus, A2317 is 20% overabundant in late-type galaxies as compared with present-day clusters.

Of the blue population, a majority (46%) are Sp/Irr with Seyfert galaxies and starbursts equally split for the remainder. The red population is primarily E/S0's (64%) with 15% classed as Sp/Irr and 21% as highly reddened starburst galaxies. Ignoring the low-luminosity starbursts, the ratio of E/S0's to red Sp/Irr's is exactly the same as present-day clusters (i.e., 4:1). This leads us to speculate that the current starburst population fades to develop into the faint *dE/dI* population that so dominates present-day cluster counts. The ratio of the remaining bright galaxies will then match the morphological fractions of present-day clusters.

The large number of Seyfert galaxies in A2317 is anomalous for a rich cluster environment. The fraction of Seyfert galaxies found in local clusters is extremely low, less than 1% (Dressler & Shectman 1988), and the fraction found in the local field is less than 2% (Huchra & Burg 1992) compared to our observed value of 11% for A2317. However, this value is similar to the fraction of AGN galaxies in 3C 295 ($z = 0.465$, $f_B = 0.22$; Dressler & Gunn 1983), and a recent study by Sarajedini et al. (1996) finds the fraction of AGNs in the field to be 10% between $z = 0.2$ and 0.6. Thus, our value of 10% is an exact match with the sharp increase of AGN activity at these redshifts in both cluster and field environments.

3.2. *Color-Magnitude Diagram*

The color-magnitude (C-M) diagrams for colors ($bz - yz$) and ($vz - yz$) are shown in Figures 3 and 4. Immediately obvious are the distinct C-M relationships for ellipticals and S0's. The C-M relation for a single burst stellar population, such as ellipticals and S0's, is a reflection of the mass-metallicity correlation predicted by simple closed-box models of galaxy evolution (Faber 1973; Tinsley 1980). The greater the mass of a galaxy, the higher its luminosity and its SN rate. The higher SN rate results in a more rapid initial enrichment of the first generation of stars and, therefore, a redder red giant branch for the composite population. The *vz* filter is located over several strong metal lines in an old population spectrum and, thus, the ($vz - yz$) colors are more sensitive to metallicity changes compared to ($bz - yz$). This can be seen in Figure 3, ($bz - yz$) versus m_{5500}, were the E/S0 sequence is effectively independent of continuum color. On the other hand, Figure 4, the ($vz - yz$) versus m_{5500} diagram, displays a clear trend of redder metallicity color with higher luminosity (mass).

The solid lines in Figures 3 and 4 are the C-M relations from local populations discussed in Schombert et al. (1993). The ($bz - yz$) relation exactly matches the A2317 galaxies,

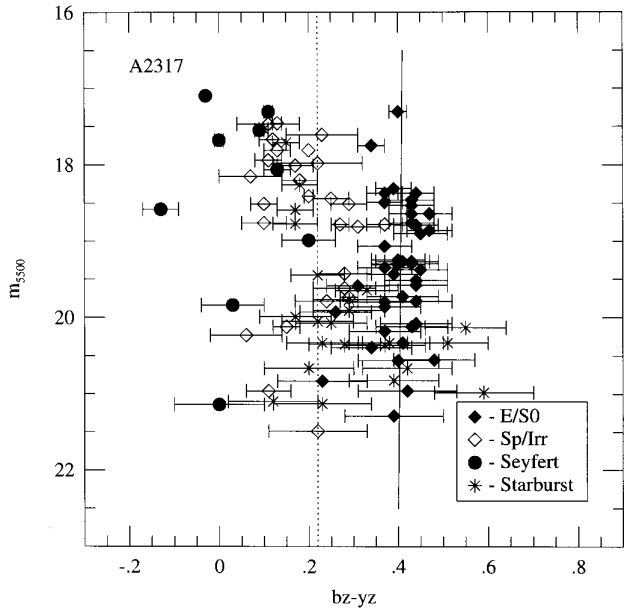

FIG. 3.—Color-magnitude diagram for the continuum color, ($bz - yz$). An L^* galaxy has an apparent mag of 19.5 ($H_0 = 50$). Photometric classifications are shown. The dotted line is the cutoff of $bz - yz = 0.22$ for blue and red galaxies. The solid line is the C-M (mass-metallicity) relation for E/S0's from Schombert et al. (1993). Note that the brightest galaxies are blue and mostly galaxies with normal star formation rates (Sp/Irr).

whereas the E/S0's appear to have a sharper slope in the ($vz - yz$) diagram. There is no direct reason for believing that the slope of the C-M relation should change dramatically with redshift. There will certainly be changes in luminosity with the galaxy population; for example, Schade (1996) finds that the surface brightness increases to 1.5 mag for an elliptical population at $z = 0.6$. However, changes in luminosity of up to 0.5 mag in Figure 4 would be unde-

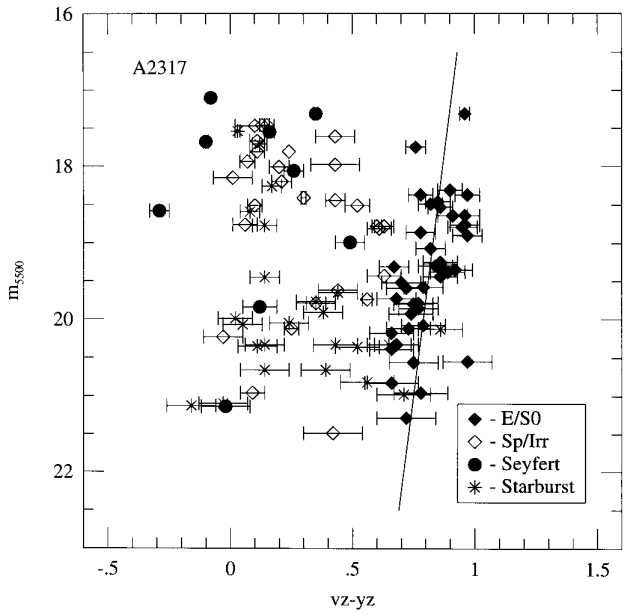

FIG. 4.—Color-magnitude diagram for the metallicity color, ($vz - yz$). Photometric classifications are shown. The solid line is the C-M (mass-metallicity) relation for E/S0's from Schombert et al. (1993). There is little change in the mass-metallicity relation for this cluster relative to the local population.

tectable in the data, since the correlation is nearly parallel to apparent magnitude. A steeper slope could suggest an age difference between low- and high-luminosity E/S0's (Bender, Saglia, & Ziegler 1996); however, there is no evidence of changes in the C-M slope in clusters at $z = 0.4$ (Oemler, Dressler, & Butcher 1997).

The blue sides of the C-M diagrams are populated with Sp/Irr's, Seyfert galaxies, and a few starburst systems. Unlike other Butcher-Oemler clusters at this redshift, a majority of the brightest galaxies are blue (see the next section). The Seyfert galaxies are scattered amongst the brightest Sp/Irr's; however the starburst systems tend to be lower in luminosity than the other galaxy types. The starburst systems also spread across a range of colors, as would be expected from their variable reddening.

3.3. *Butcher-Oemler Effect*

The original broadband definition of the fraction of blue to red galaxies, f_B, given by Butcher & Oemler (1984), is the ratio of galaxies 0.2 mag bluer than the mean color of the E/S0 sequence (after K-corrections) to the total number of galaxies in the cluster. As discussed in Rakos et al. (1990), a sample of nearby spirals and irregulars is used to determine a value of $(bz - yz)$ (continuum color) in our filter system that separates star-forming from quiescent galaxies. From this previous analysis, we have defined the fraction of blue galaxies, f_B, as the ratio of the number of galaxies bluer than $(bz - yz) = 0.22$ to the total number of galaxies. Since the mean $(bz - yz)$ color of a present-day elliptical is 0.37 (Schombert et al. 1993) and $(bz - yz)$ maps into $(B-V)$ in a linear fashion with a slope of 1.33 (Matsushima 1969), then a cut at $(bz - yz) = 0.22$ is effectively the same as Butcher & Oemler's 0.2 mag selection, and the two values are directly comparable. In fact, we have argued that our narrowband system is superior to the broadband $(B-V)$ criteria owing to our filters' unique locations on continuum regions of a galaxy's SED. The interpretation of the Butcher-Oemler effect within our filter system is a comparison of the mean temperature of the composite stellar photosphere, undistorted by emission lines or foreground/background contamination.

Applying this criteria to A2317 produces an f_B value of 0.35 ± 0.06, which for this redshift range makes it a cluster unusually rich in blue galaxies (note that a typographical error in RS95 lists A2317 with a f_B value of 0.51; the correct value is 0.31 for that study, which is well within the errors of this current, deeper data set). Figure 3 shows a dashed line for the $(bz - yz)$ cutoff for red/blue classification. Note that all the E/S0 type galaxies from the photometric classification are within the red boundary. This does not imply that the poststarburst "E + A" type galaxies are missing from A2317. This type of galaxy is a mismatch of morphology with color (a smooth morphology with a blue underlying stellar population suggestive of recent star formation) and would have been classed as an Sp/Irr in our system. Nine Sp/Irr's also lie within the red population region, which demonstrates that a simple color division of a cluster population can overlook a more subtle variation in multicolor space. These objects are most likely early-type spirals with large bulges that dominate the colors but with small star-forming disks that are still detectable in our multicolor space. There is also the possibility that these galaxies are young S0's with poststarburst disks (Bothun & Gregg 1990). Numerous starburst class galaxies also lie within the red region; however inspection of Figure 2 shows that these are all simply very reddened systems.

Figures 3 and 4 also show that the brightest galaxies have bluest colors. In fact, the measured f_B value for the cluster is strongly dependent on the cut-off magnitude of the sample. This can be seen in Figure 5, which displays f_B as a function of m_{5500}. The fraction of blue galaxies is over 75% in the highest magnitude bin, dropping to only 10% for galaxies with luminosities between L^* and $\frac{1}{2}L^*$ and then rising again for galaxies with luminosities below $\frac{1}{2}L^*$. The change in f_B is significant and implies that the scatter in the Butcher-Oemler effect with redshift (see Fig. 4 of RS95), particularly at low redshifts, may be due to limiting magnitude effects combined with evolutionary changes in the luminosity function with redshift. For example, the brightest blue galaxies may have very short lifetimes, not in terms of existence as self-gravitating entities, but in terms of visibility. In RS95, a scenario was proposed in which Butcher-Oemler galaxies fade into LSB galaxies or low-luminosity dwarf galaxies after their initial burst of star formation. There is some evidence of this effect in other cluster studies (see Schade 1996) in that blue galaxies in distant clusters display a measured increase of 1–1.5 mag in mean surface brightness.

The rise in f_B at the lowest luminosities in A2317 is suggestive of an increasing contribution from a dwarf galaxy population. Although this luminosity range is not completely sampled by our study, the minimum in f_B at 19.5 (see Fig. 5) is also at the same absolute luminosity at which, in the Virgo Cluster, there is a shift in the luminosity function from giant galaxies to a high fraction of dwarf Irr, Im, and Sm's. The class of dE galaxies dominates the luminosity function at very low luminosities (Sandage, Binggeli, & Tammann 1985), but blue late-type systems at just below L^* are sufficiently numerous to produce a rise in the blue galaxy fraction. We note that most of the galaxies classified as starburst are in the lower luminosity bins. Although many of the starburst galaxies are not blue galaxies because of reddening effects, the larger fraction below L^* would lend support to the proposal of Koo et al. (1997) that a majority

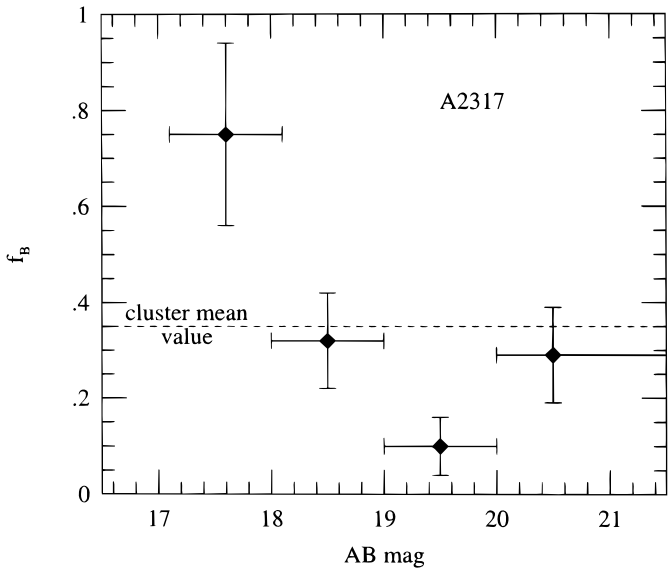

FIG. 5.—The fraction of blue galaxies, f_B, as a function of absolute magnitude. The highest fraction of blue galaxies are also the brightest members of the cluster. The rise at faint luminosities signals the increasing contribution from low-mass dwarfs and late-type Irr/Im/Sm types.

of the starburst systems in clusters at intermediate redshifts are dwarf galaxies undergoing a phase of star formation. These bursting dwarfs would have a relatively high luminosity for a short time period, then fade to normal dwarf luminosities by the present epoch.

Although the morphological type of the brightest blue galaxies is not known (our photometric classification does not distinguish between early and late-type spirals), results from recent *HST* imaging of distant clusters suggests that these systems are structurally late-type spirals (i.e., they have small B/D ratios) with slightly increased levels of star formation activity (Oemler et al. 1997). Along the same lines, the galaxies photometrically classified as starburst can linked with the merging/interacting systems found by the Oemler et al. (1997) study. The average merging/interacting systems in the four clusters from Oemler et al. is 17%, compared with the 22% fraction of starburst galaxies in A2317, which is in agreement with our expectation that the strongest star formation in this Butcher-Oemler cluster is tidally induced (see below). Regardless of the appearance of either the Sp/Irr or the starburst galaxies, the main conclusion from Figure 4—that the blue Butcher-Oemler population is primarily composed of galaxies with normal star formation rates typical of present-day spirals and irregulars—is in agreement with the morphological studies.

3.4. *Galaxy Harassment and the Origin of the Blue Population*

The spatial distribution of blue and red galaxies is shown in Figure 6, which is a histogram of number density (normalized by projected area) as a function of radius from the cluster core. In this figure, the cluster core is calculated from the geometric mean of the photometrically determined cluster members. The results below were insensitive to changes in the center at the level of 20″. Immediately obvious from Figure 6 is that the red galaxies have the highest densities at the cluster center and have a smooth density dropoff toward the outer part of the cluster. In contrast, the blue galaxies have a marked drop in their density for the inner third of the cluster with a roughly uniform spatial density in the outer part of the cluster. There is no obvious trend between Sp/Irr, Seyfert, or starburst types.

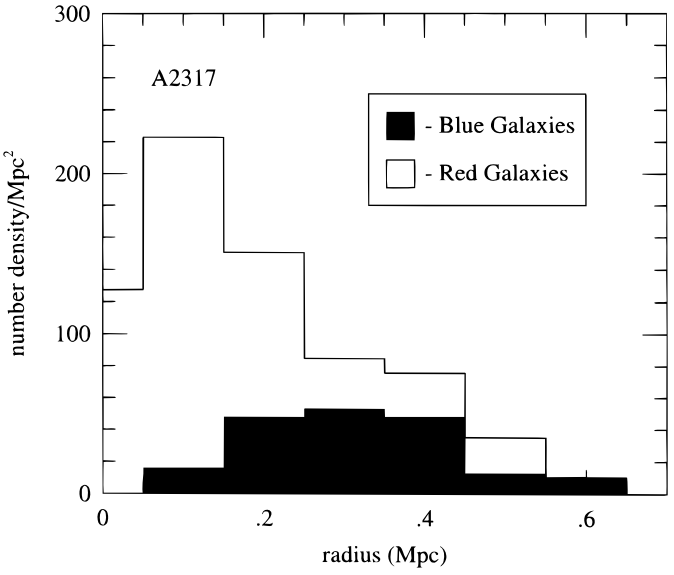

FIG. 6.—The number density of blue and red galaxies as a function of cluster radius. The red population dominates the core of the cluster with the blue population having a marked decrease inside 0.3 Mpc. This is in agreement with one of the predictions of "galaxy harassment" models, where the blue population is due to tidally induced star formation from the cluster and the most massive members.

The blue population has long been suspected of avoiding the densest regions of a cluster core (see Dressler 1993), and a recent study by Abraham et al. (1996) has shown a distinct drop in f_B toward the core of A2390, which is another Butcher-Oemler cluster. Carlberg et al. (1997), in a study of the CNOC cluster sample, demonstrate that not only is there a drop in the blue galaxy fraction at cluster cores, but the red population has a smaller velocity dispersion by a factor of 1.3 compared with the blue population.

The difference in the red and blue population dynamics has led Abraham et al. (1996) to propose that the Butcher-Oemler effect is due to an infalling field population. The subsequent dying out of the blue population is caused by truncation of star formation from stripping by the intracluster medium. The infalling spirals then evolve into red S0's, which is in agreement with the large fraction of S0's found in present-day clusters. Unfortunately, the *HST* morphological data does not agree with this scenario in the sense that the blue population is shown to be composed of small-bulge, late-type spirals that will not fade into large-bulge S0's. The argument made in Abraham et al. (1996) is that the relevant parameter is the ratio of the bulge luminosity to disk luminosity, which will change dramatically with the cessation of star formation in the disk. Of course, the bulge-to-disk ratio is only one component of the morphological classification of spirals (the other two components are tightness of spiral arms and degree of resolution of the arms into stars), so the question of whether the Butcher-Oemler population evolves from late-type to early-type will remain unresolved until a detailed surface photometric decomposition of the blue galaxies is made.

If Oemler et al. (1997) have correctly classified the blue galaxy population as late-type spirals with small bulges, then the origin and destiny of the Butcher-Oemler galaxies remains unclear. The high fraction of mergers/interactions is suggestive of tidally induced star formation, yet this does not resolve the fate of the blue galaxies, since even the abrupt cessation of star formation would still leave a population of red, late-type spirals in present-day clusters, which is not seen. Tidal interactions may well explain the high fraction of starburst galaxies; these would have their origin in gas-rich dwarf galaxies undergoing a short, but intense, tidally induced starburst (Koo et al. 1997). It should be noted, however, that the cluster environment is the most surprising arena for the type of interactions that can lead to star formation bursts. The orbits of cluster galaxies are primarily radial, and the typical velocities are high. This makes any encounter with another galaxy short-lived, with little impulse being transferred as required to shock the incumbent molecular clouds into a nuclear starburst.

Recently, a new mechanism for cluster-induced star formation has been proposed. This method, called galaxy harassment (Moore et al. 1996), emphasizes the influence of the cluster tidal field and rapid, impulse encounters with massive galaxies. These two processes conspire to not only raise the luminosity of cluster spirals, but also to increase their visibility and hence their detectability. One of the predictions of galaxy harassment is that galaxies in the cores of clusters will be older than galaxies at the edges. In terms of

star formation history, this is exactly what Figure 6 has demonstrated in A2317. The blue population (i.e., the harassed population) is primarily located in the outer two-thirds of the cluster. Other explanations of the blue population, such as ram pressure stripping or infall of blue galaxy–rich subclusters, would have the blue population primarily confined to the cluster edges.

3.5. *Fate of the Butcher-Oemler Population*

Regardless of the origin of the blue population, its fate is obvious. These galaxies do not exist in present-day clusters and, therefore, must either be destroyed or reduced to the luminosity of dwarf galaxies. Two points concerning A2317 make this fate difficult to reconcile with our current understanding of galaxy evolution. The first is that the Butcher-Oemler population is numerous, and the second is that this population contains many bright members. Despite any changes in total luminosity or surface brightness, the blue population makes up a significant fraction of a cluster numerically, and this value increases with redshift. Since our survey of present-day clusters is complete to extremely low luminosity and surface brightness, this implies that the blue population must eventually be eliminated as recognizable units or transformed into objects with much smaller luminosity. This conclusion is supported by the observation derived from Table 1 that the red population already contains the correct morphological mix found in local clusters. A conversion of blue to red galaxies is not needed to resolve morphological distributions.

One point to remember is that the destruction of the Butcher-Oemler population is only a radical proposition if these galaxies contain a significant fraction of the mass of the cluster rather than luminosity. For example, the blue population may be a specific population of objects with very low M/L's or extremely short lifetimes. Some of the blue population may be bursting dwarf galaxies, as proposed by Koo et al. (1997) and as suggested by the population of low-luminosity starbursts in this study; however, the *HST* imaging results indicate that most of the blue population, particularly the bright objects, are normal late-type spirals by their morphological appearance.

Interestingly enough, there already exists a class of galaxies that combines late-type morphological appearance with a particular frailty to tidal forces. These are the LSB galaxies of recent attention in field surveys and dark matter investigations (see Impey & Bothun 1997 for a review). Recent work has shown that LSB galaxies, which are by definition low in luminosity density, are gas-rich and low in mass density (de Blok & McGaugh 1996). Thus, LSB galaxies would be particularly susceptible to tidally induced star formation (Mihos, McGaugh, & de Blok 1997). LSB galaxies also have an unusually high incidence of low-luminosity AGN activity (Impey & Bothun 1997), which may account for the large number of Seyfert galaxies in our sample, as starburst gas is also dumped onto a central engine.

The scenario proposed here is similar to the one we proposed in RS95, that the Butcher-Oemler population is an evolved set of LSB galaxies. The mechanism of galaxy harassment or ram pressure induces highly efficient star formation in these dark matter systems that increases their visibility and actual luminosity. Later encounters with the cluster core destroys this low-mass density system by tidal forces. Thus, we believe that the Butcher-Oemler cluster will evolve into future cD clusters from the released stellar material of the disrupted LSB population.

4. SUMMARY

This paper has presented deep multicolor photometry of the intermediate redshift cluster A2317. The color system used herein is a specific form of the Strömgren color system, matched to the rest frame of A2317, in order to understand the components of the blue Butcher-Oemler population known to inhabit this cluster. Our primary results are summarized as follows:

1. One hundred twelve cluster members were identified and classified by our photometric system with four subtypes: (1) E/S0, (2) Sp/Irr, (3) Seyfert, or (4) starburst. The fractional population is listed in Table 1, and color diagrams are shown in Figures 1 and 2. The fraction of blue galaxies is $f_B = 0.35$.
2. The C-M diagrams in Figures 3 and 4 show that the blue population dominates the top and bottom of the luminosity function. That is to say, the brightest galaxies are blue, with a decrease at intermediate magnitudes, then a rise at low luminosities (see Fig. 5). There is a steepening of the C-M relation for E/S0's as compared to the locally determined relation, but the difference is not statistically significant within the context of only one cluster determination.
3. The Butcher-Oemler population is, based on our photometric classification system, primarily a population of galaxies with normal star formation rates. Although there are anomalously high fractions of Seyfert galaxies and starburst galaxies in A2317, most of the blue galaxies are classified as Sp/Irr. The starburst systems tend to be of low luminosity, which suggests that they may be bursting dwarfs (Koo et al. 1997). The above photometric classification of the Butcher-Oemler population, based on their star formation history, is in agreement with their *HST* image classifications as late-type spirals (Oemler et al. 1997).
4. The spatial location of the blue population (see Fig. 6) indicates that the Butcher-Oemler effect is confined to the outer cluster regions with the red population dominating the cluster core. This result is in agreement with the prediction of galaxy harassment models, where the cluster tidal field and impulse encounters with more massive galaxies results in tidally induced star formation or infall models of spiral-rich, merging subclusters.

The fate of the Butcher-Oemler population is still undetermined, since they are too numerous and too recent to simply fade from view by the present epoch. We renew our arguments that the most plausible fate for the blue population is destruction and that the Butcher-Oemler population is composed of low-density LSB galaxies that are particularly susceptible to disruption in the dense cluster cores.

The authors wish to thank the director and staff of KPNO and Steward Observatory for granting time for this project. Financial support from the Austrian Fonds zur Förderung der Wissenschaftlichen Forschung is gratefully acknowledged. This research has made use of the NASA/IPAC Extragalactic Database (NED), which is operated by the Jet Propulsion Laboratory, California Institute of Technology, under contract with the National Aeronautics and Space Administration.

REFERENCES

Abell, G., Corwin, H., & Olowin, R. 1989, ApJS, 70, 1
Abraham, R., et al. 1996, ApJ, 471, 694
Bender, R., Saglia, R., & Ziegler, B. 1996, The Early Universe with the VLT, (ESO Workshop), ed. J. Bergeron (Berlin: Springer), 1
Bothun, G., & Gregg, M. 1990, ApJ, 350, 73
Butcher, H., & Oemler, A. 1984, ApJ, 285, 426
Carlberg, R., et al. 1997, ApJ, 476, L7
de Blok, E., & McGaugh, S. 1996, ApJ, 469, 89
Donnelly, H. 1994, in Clusters of Galaxies, ed. F. Durret, A. Mazure, & J. Tran Thanh Van (Paris: Editions Frontières), 39
Dressler, A. 1993, ASP Conf. Ser. 51, Observational Cosmology Symposium, ed. C. Chincarini, A. Iovino, T. Maccacro, & D. Maggagni (San Francisco: ASP), 225
Dressler, A., & Gunn, J. 1983, ApJ, 270, 7
Dressler, A., & Shectman, S. 1988, AJ, 95, 985
Ellis, R. 1997, ARA&A, 35, 345
Faber, S. 1973, ApJ, 179, 731
Fiala, N., Rakos, K., & Stockton, A. 1986, PASP, 98, 70
Huchra, J., & Burg, R. 1992, ApJ, 393, 90
Impey, C., & Bothun, G. 1997, ARA&A, in press
Koo, D. 1986, ApJ, 311, 651
Koo, D., Guzman, R., Gallego, J., & Wirth, G. 1997, preprint, astro-ph/9701119
Lehnert, M., & Heckman, T. 1996, ApJ, 472, 546
Matsushima, S. 1969, ApJ, 158, 1137
Mihos, J., McGaugh, S., & de Blok, E. 1997, ApJ, 477, 79
Moore, B., Katz, N., Lake, G., Dressler, A., & Oemler, A. 1996, Nature, 379, 613
Oemler, A. 1992, in Clusters and Superclusters of Galaxies, ed. A. Fabian (Dordrecht: Kluwer), 666
Oemler, A., Dressler, A., & Butcher, H. 1997, ApJ, 474, 561
Oke, J., & Gunn, J. 1983, ApJ, 266, 713
Rakos, K., Fiala, N., & Schombert, J. 1988, ApJ, 328, 463
Rakos, K., Maindl, T., & Schombert, J. 1996, ApJ, 466, 122 (RMS96)
Rakos, K., & Schombert, J. 1995, ApJ, 439, 47 (RS95)
Rakos, K., Schombert, J., & Kreidel, T. 1990, ApJ, 377, 382
Sarajedini, V., Green, R., Griffiths, R., & Ratnatunga, K. 1996, ApJ, 471, L15
Sandage, A., Binggeli, B., & Tammann, G. 1985, AJ, 90, 1759
Schade, D. 1996, preprint, astro-ph/9612170
Schombert, J., Hanlan, P., Barsony, M., & Rakos, K. 1993, AJ, 106, 923
Tinsley, B. 1980, Fundam. Cosmic Phys., 5, 287
Tyson, J. 1988, AJ, 96, 1